22. J. F. Kelly, K. G. Horton, *Glob. Ecol. Biogeogr.* **25**, 1159–1165 (2016).

ACKNOWLEDGMENTS

G.H.'s visiting scholarship was funded by the China Scholarship Council. We acknowledge the support provided by COST—European Cooperation in Science and Technology through the Action ES1305 "ENRAM." The project was supported by UK Biotechnology and Biological Sciences Research Council grant BB/J004286/1 to J.W.C. Data are available at Dryad at http://dx.doi.org/10.5061/dryad.6kt29.

SUPPLEMENTARY MATERIALS

www.sciencemag.org/content/354/6319/1584/suppl/DC1
Materials and Methods
Figs. S1 to S8
Tables S1 to S8
References (*23*–*49*)

27 June 2016; accepted 22 November 2016
10.1126/science.aah4379

BRAIN RESEARCH

Active cortical dendrites modulate perception

Naoya Takahashi,[1] Thomas G. Oertner,[2] Peter Hegemann,[3] Matthew E. Larkum[1]*

There is as yet no consensus concerning the neural basis of perception and how it operates at a mechanistic level. We found that Ca^{2+} activity in the apical dendrites of a subset of layer 5 (L5) pyramidal neurons in primary somatosensory cortex (S1) in mice is correlated with the threshold for perceptual detection of whisker deflections. Manipulating the activity of apical dendrites shifted the perceptual threshold, demonstrating that an active dendritic mechanism is causally linked to perceptual detection.

Recent studies in awake rodents indicate that dendritic Ca^{2+} activity in L5 cortical pyramidal neurons is elevated during cognitive processes (*1*–*4*). These studies are in line with the proposal that the Ca^{2+} electrogenic properties of the apical dendrites of pyramidal neurons (*5*, *6*) amplify the effects of feedback inputs [apical amplification (*7*)] to superficial cortical layers (*8*, *9*). There is evidence for the crucial role of feedback to primary sensory regions in perceptual processes (*11*, *12*), but it still remains to be demonstrated experimentally that perception depends on a dendritic mechanism. We reasoned that the decisiveness of this mechanism could be tested by examining dendritic Ca^{2+} activity around the perceptual threshold that corresponds to the transition from subliminal to liminal perception in humans (*13*). The apical amplification hypothesis predicts that dendritic Ca^{2+} activity in a subset of neurons correlates to this transition, leading to the detection of stimuli (Fig. 1A). To test this experimentally, we used a whisker-based tactile detection task in mice (*10*) combined with two-photon Ca^{2+} imaging of pyramidal apical dendrites in S1. Additionally, we investigated the causal relationship between dendritic Ca^{2+} and perceptual detection by testing whether manipulating dendritic Ca^{2+} currents alters detection.

Animals were first trained to report whisker deflections by licking to obtain water rewards (Fig. 1, B and C). The C2 whisker was selectively stimulated using a magnetic coil (fig. S1). The mice learned the task (>80% correct "hit" responses), with low false alarm rates (i.e., the licking rate at zero stimulus intensity), within 2 weeks, at which point we determined the psychometric function for whisker stimulation by using a range of intensities above and below the perceptual detection threshold (Fig. 1D). The perceptual detection threshold for individual animals was determined by fitting the psychometric function with a sigmoid function (*14*) (Fig. 1E). The behavioral thresholds remained at the same level across sessions over days (Fig. 1F). The delay between the whisker deflection and an animal's reaction (first lick) in "hit" trials was shorter in the trials of salient stimuli than in threshold stimuli (Fig. 1G).

We simultaneously performed fast-scanning two-photon Ca^{2+} imaging from apical dendrites of L5 neurons in the C2 barrel column in primary somatosensory cortex (S1) (Fig. 1H). In each field of view (175 by 175 μm), 98.1 ± 17.8 apical dendrites were identified at 200 to 300 μm below the pia (mean ± SD, n = 8 sessions from 8 mice). During the behavior, large Ca^{2+} transients were observed in some apical dendrites after whisker deflections (Fig. 1I). To investigate the relationship between dendritic activity and perceptual behavior of the animal, Ca^{2+} responses were determined for seven different stimulus intensities around the behavioral threshold (Fig. 1I, vertical columns). We compared the activity in "lick" trials (Fig. 1I, lower rows) to "no-lick" trials (upper rows) and averaged the responses over all trials (bottom traces).

How does dendritic Ca^{2+} relate to behavior for this whisker detection task? To examine this, we plotted the dendritic Ca^{2+} response as a function of stimulus intensity—i.e., the neurometric function—versus detection probability as a function of stimulus intensity—i.e., the psychometric function (Fig. 2A, right). In some cases, the increase in dendritic Ca^{2+} closely followed the behavioral performance of the animal (Fig. 2A). Interestingly, in a smaller fraction of cases, we found the opposite: dendritic Ca^{2+} anticorrelated with stimulus strength (Fig. 2A), which may be indicative of a parallel coding scheme such as predictive coding (*15*). The correlation of dendritic Ca^{2+} to behavior was quantified using a similarity index (SI) (*16*) and compared to chance level by shuffling the stimulus intensities of the original data (Fig. 2B). In 34% (267 of 785) of cases, the SIs deviated from chance. The fraction of dendrites responding to salient whisker deflections was greater in mice engaged in the task than naïve (untrained) mice (fig. S2).

We also investigated the discriminability of dendritic Ca^{2+} by evaluating the behavioral outcome (hit or miss) versus the Ca^{2+} response near the threshold for behavior—i.e., the discrimination index (DI) based on a receiver operating characteristic (ROC) analysis (*17*) (Fig. 2C) (also see methods in the supplementary materials). In 22% (173 of 785) of dendrites, the dendritic Ca^{2+} near threshold alone could be used to predict the behavior with prolonged increases in Ca^{2+} signals in "lick" trials, but not in "no-lick" trials (Fig. 2D, *DI > 0, $P < 0.05$; and Fig. 2E, left). Again, in some neurons (68 of 785), the behavior was predicted by a decrease in dendritic Ca^{2+} (Fig. 2D, *DI < 0, $P < 0.05$; and Fig. 2E, right). In another group of neurons with high SIs and low DIs, evoked Ca^{2+} signals increased with increasing amplitudes of whisker deflection but were independent of behavioral outcome, suggesting that these neurons coded for information orthogonal to perceptual detection (Fig. 2E, middle). We characterized the temporal and spatial features of perception-relevant dendrites (DI's $P < 0.05$). The timing of the dendritic Ca^{2+} increases for high stimulus strengths was faster than that for near-threshold stimuli, and the dendritic Ca^{2+} mostly preceded the behavior (Fig. 2F and fig. S3). We found a small but significant relationship between the physical location of the dendrites and their DI (Fig. 2, G and H).

Activation of dendritic Ca^{2+} channels results in enhanced firing of individual L5 pyramidal neurons in vivo (*18*). We monitored the firing activity of L5 neurons while the animal performed the whisker detection task (Fig. 3A). The results of 40 cells recorded from L5 (depth, 577.8 to 774.0 μm below the pia) in behaving animals were pooled. Mean firing rates were 11.1 ± 14.2 Hz, ranging from 0.68 to 63.1 Hz (mean ± SD, n = 40 cells from 10 mice). In a fraction of neurons, perceived whisker stimuli increased firing activity, resulting in positive correlations between neurometric and psychometric functions (Fig. 3B). As seen in dendritic Ca^{2+} activity, we also observed some cells for which the firing activity

[1]Institute for Biology, Neuronal Plasticity, Humboldt Universität zu Berlin, D-10117, Berlin, Germany. [2]Institute for Synaptic Physiology, University Medical Center Hamburg-Eppendorf, D-20251, Hamburg, Germany. [3]Institute for Biology, Experimental Biophysics, Humboldt Universität zu Berlin, D-10115, Berlin, Germany.
*Corresponding author. Email: matthew.larkum@hu-berlin.de

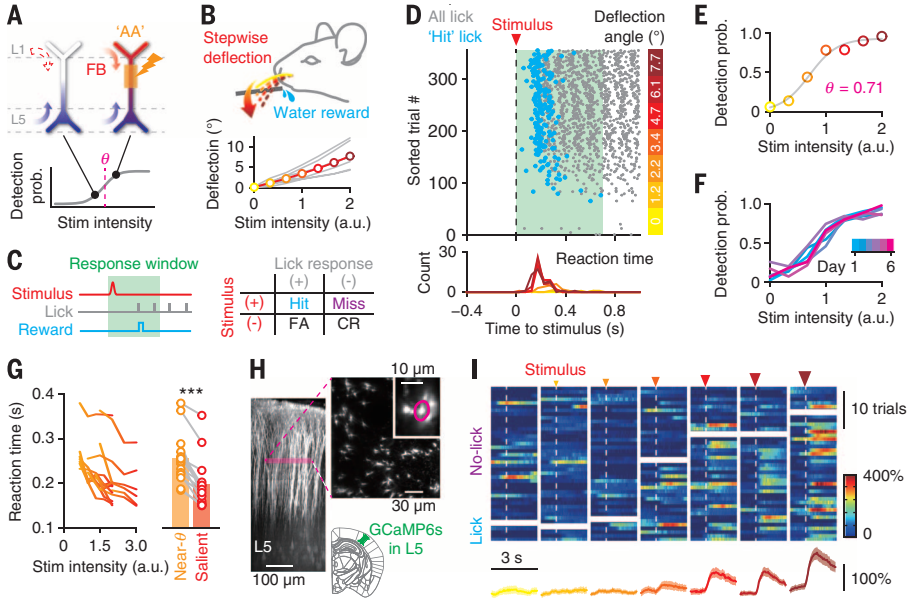

Fig. 1. Behavior perceptual detection threshold for a whisker detection task. (**A**) Apical amplification (AA) hypothesis (*7*) in a sensory detection paradigm. Above the perceptual detection threshold, in addition to feed-forward information (blue arrows), pyramidal neurons in primary sensory cortex receive long-range feedback (FB) (red arrow) inputs from other cortical regions arriving at distal tuft dendrites. Active dendritic Ca^{2+} currents conjugate early sensory with feedback information (*6*), leading to sensory perception. (**B**) (Top) Behavioral task design. (Bottom) Deflection angle of whisker is proportional to stimulus intensity. Mean amplitude (color) plotted with individual data (gray) (n = 7 mice) (see also fig. S1). (**C**) Stimulus paradigm (left) and table of behavioral outcomes classified into four categories–i.e., hit, miss, false alarm (FA), and correct rejection (CR) (right). (**D**) (Top) Raster plot of lick events (gray) in 357 trials from a single session sorted by intensity of the presented stimulus. Rewarded (hit) licks marked in blue. (Bottom) Histograms of response timings of first lick at different stimulus intensities. (**E**) Psychometric function for the behavioral performance shown in (D). (**F**) Psychometric functions over 6 days, obtained from the same mouse. (**G**) (Left) Reaction times for stimuli above thresholds plotted as a function of stimulus intensity (n = 15 sessions from 15 mice). (Right) Reaction times for near-threshold stimuli and salient (maximum) stimuli. (**H**) Two-photon Ca^{2+} imaging from the apical dendrites of L5 neurons expressing GCaMP6s (left) in the C2 barrel column (bottom right). (Inset) Horizontal imaging plane (216 µm from pia). (**I**) Ca^{2+} signals in an apical dendrite marked in (H) during the detection task organized according to increasing stimulus intensity (columns) and trials (rows), separated based on the behavioral response ("lick" or "no-lick") by a blank row. (Bottom) Average and SEM of Ca^{2+} responses for all trials of a given stimulus intensity.

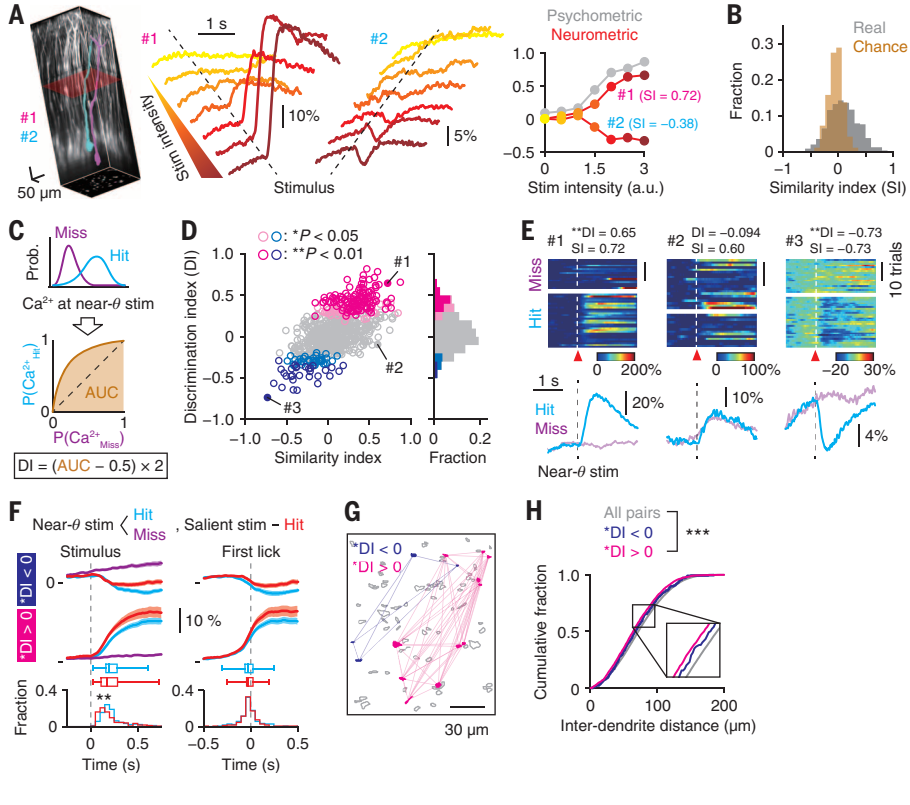

Fig. 2. Apical dendritic Ca^{2+} activity during the perceptual detection task. (**A**) (Left) Three-dimensionally reconstructed apical dendrites (#1 and #2) in the same field of view. Imaging plane is shown in red. (Middle) Averaged Ca^{2+} responses to various stimulus intensities from the two different apical dendrites. (Right) Neurometric functions of the dendritic Ca^{2+} activities compared with behavioral performance (psychometric function). (**B**) Correlation between neurometric and psychometric functions evaluated by the similarity index (SI) based on Euclidean distance. Distribution of SIs from real data (gray) compared with chance level (brown). (**C**) Schematic of ROC analysis (*17*): The discrimination index (DI)—the likelihood that dendritic Ca^{2+} activity predicted the animal's detection of near-threshold stimuli—estimated based on the area under the ROC curve (AUC). (**D**) (Left) Dendritic responses characterized by SIs and DIs. Dendrites with high discriminability shown in color. Statistical significance of DI was computed by a permutation test. (Right) Histogram of DIs. (**E**) (Top) Examples of individual dendritic Ca^{2+} responses for near-threshold stimuli for the three cases in (D). (Bottom) Average Ca^{2+} activity during hit (blue) and miss (purple) trials. (**F**) (Top) Timing of the Ca^{2+} response to near-threshold and salient stimuli in discriminatory dendrites (*P < 0.05) aligned by the onsets of the stimuli (left) or by the timing of an animal's first (rewarded) licks (right). Average traces shown with SEM (n = 173 dendrites for *DI > 0, n = 68 dendrites for *DI < 0). (Bottom) Histograms of onset timings of Ca^{2+} responses in dendrites with *DI > 0 to near-threshold and salient stimuli in hit trials (stimulus-aligned, **$P = 9.7 \times 10^{-3}$; first lick–aligned, P = 1.0, Kolmogorov-Smirnov test). (**G**) Spatial distribution and interdendritic distance of imaged dendrites (outlined) in a single field of view with discriminatory dendrites denoted by color. (**H**) Cumulative fraction of dendritic pairs as a function of distance between imaged dendrites (n = 39,232 pairs, gray), dendrites with *DI > 0 (n = 2456 pairs, magenta), and dendrites with *DI < 0 (n = 319 pairs, blue) (all pairs versus *DI > 0, ***$P = 4.2 \times 10^{-14}$, Kolmogorov-Smirnov test).

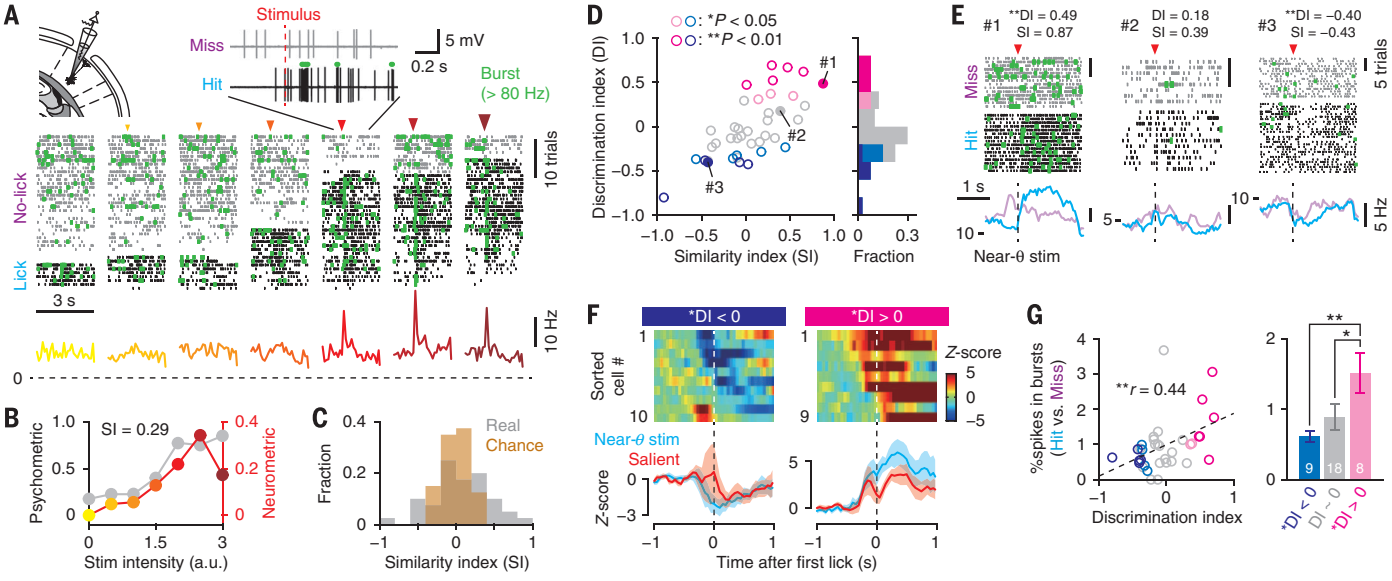

Fig. 3. Firing behavior of L5 neurons during the perceptual detection task. (**A**) (Top) Juxtacellular recording from behaving animals. (Middle) Raster plot of the firing activity of an L5 neuron in the C2 barrel column. Green dots in (A) and (E) indicate spikes in burst events (>80 Hz). (Bottom) Peristimulus spike time histograms (PSTHs). (**B**) Neurometric function of the neuron in (A) compared with the psychometric function. (**C**) Distribution of similarity indices (SIs) between neurometric and psychometric functions. (**D**) Firing responses of recorded neurons were characterized by SI and DI, as in Fig. 2D. (**E**) Example raster plots and PSTHs of firing responses of L5 neurons to near-threshold whisker stimuli for the three cases in (D). (**F**) (Top) Normalized firing responses to near-threshold and salient stimuli in neurons with high discriminability (DI's $*P < 0.05$) aligned by the timing of behavioral reaction (first lick). (Bottom) Average PSTHs shown with SEM. (**G**) (Left) The proportion of spikes in bursts [i.e., green versus black/gray dots in (E)] for near-threshold stimuli in hit trials relative to miss trials as a function of DI (Pearson's correlation coefficient $r = 0.44$, $**P = 8.7 \times 10^{-3}$). (Right) Average proportional bursting for hit versus miss, shown with SEM for discriminatory neurons (*DI < 0, *DI > 0) and nondiscriminatory neurons (DI ~ 0) ($**P < 0.01$, $*P < 0.05$, Dunn's test after Kruskal-Wallis test).

negatively correlated to animal behavior. In 38% (15 of 40) of recorded cells, firing activity correlated (or anticorrelated) beyond chance to animal behavior (Fig. 3C). The same ROC analysis performed on dendritic Ca^{2+} (Fig. 2C) was used to determine the DI for the likelihood that a change in firing could predict the animal's behavior when near-threshold stimuli were given (Fig. 3, D and E). About 23% (9 of 40) of cells increased their firing activity to near-threshold stimuli preferentially in "hit" trials, whereas 25% (10 of 40) decreased their firing activity (Fig. 3D). In most cells that significantly correlated to the animal's behavior (DI's $P < 0.05$), the firing change preceded the licking reaction of the animal (Fig. 3F) (11 out of 19 neurons). The burstiness of firing correlated to discriminability (Fig. 3G), suggesting that burst firing is more salient for perceptual detection (*19*). However, burst firing was less predictive of behavior than spike rate alone. In summary, changes in firing corresponding to perceptual detection occurred in a similar proportion of L5 pyramidal neurons as observed with dendritic Ca^{2+} activity.

Our data show that dendritic Ca^{2+} signals are correlated to animals' perceptual behavior. Indeed, the timing between dendritic Ca^{2+} activity and licking behavior suggests a causal relationship (Fig. 2F and fig. S3). To investigate causality, we manipulated dendritic activity pharmacologically and optogenetically during the task. The γ-aminobutyric acid type B ($GABA_B$)–receptor agonist baclofen suppresses dendritic Ca^{2+} spikes (fig. S4) (*20*). Here, local application of baclofen to superficial layers profoundly suppressed ongoing Ca^{2+} activity in apical tufts in awake animals (Fig. 4A). On the other hand, application of baclofen in vivo does not affect sensory-evoked subthreshold activity in L5 neurons (*18*). Importantly, baclofen also strongly shifted the animals' behavioral responses to higher stimulus values (Fig. 4B, left, and fig. S6B) with the largest changes occurring at the perceptual detection threshold (Fig. 4B, right). Saline had no effect on perceptual detection (fig. S6, E to I).

We expressed a chloride-conducting channelrhodopsin (iChloC) (*21*) in L5 neurons in the C2 barrel column. Brief illumination with blue light in the superficial cortical layers induced a prolonged suppression of Ca^{2+} activity in the apical dendrites of L5 neurons expressing iChloC (Fig. 4C). Ex vivo experiments confirmed that depth-calibrated 470-nm light used in vivo effectively blocked Ca^{2+} spikes in apical dendrites without any effects on somatic excitability (fig. S5). Inactivating the superficial dendrites with iChloC also caused a significant impairment in the animals' detection probability of threshold stimuli (Fig. 4D).

We took advantage of an innate inhibitory circuit in the cortex known to down-regulate dendritic activity (*22*, *23*), the dendrite-targeting somatostatin (SOM) inhibitory cells. This circuitry has been shown to gate dendritic excitability (*4*, *24*). We therefore suppressed dendritic activity by activating SOM cells with channelrhodopsin-2 (ChR2) (Fig. 4E). Suppression of dendritic activity via SOM cell activation significantly increased the perceptual detection threshold (Fig. 4F). All of the manipulations to down-regulate dendritic activity shifted the psychometric function to the right toward higher stimulus intensities but did not alter the gain (slope) nor the false alarm rate (fig. S6) (*25*).

Finally, we tested the consequence of up-regulating apical dendrites of L5 neurons on the animals' perceptual detection. The apical dendrites of L5 neurons expressing ChR2 were photostimulated using a fiberoptic cannula, which directed the 470-nm light specifically to superficial layers in a single barrel column. This spatially confined dendritic activation efficiently shifted the detection threshold toward lower stimulus intensities (Fig. 4H and fig. S6S). Importantly, reinforced activity of apical dendrites caused an increase in false alarm rate, indicating that dendritic activity could contribute to the intrinsic generation of sensory perception (fig. S6U). Together, these results suggest that the activity in apical dendrites of L5 neurons is causally linked to the perceptual behavior of the animal.

The results presented here show that a Ca^{2+}-dependent mechanism in the apical dendrites of L5 pyramidal neurons causally influences perceptual detection (*6*). They are consistent with recent studies showing that dendritic Ca^{2+} activity is correlated with behavior (*1*, *2*, *4*). Our data show that this dendritic mechanism is activated at the crucial transition from subliminal to liminal detection and can therefore be regarded as a neural correlate for perceptual detection. Four contrasting approaches that manipulated dendritic activity

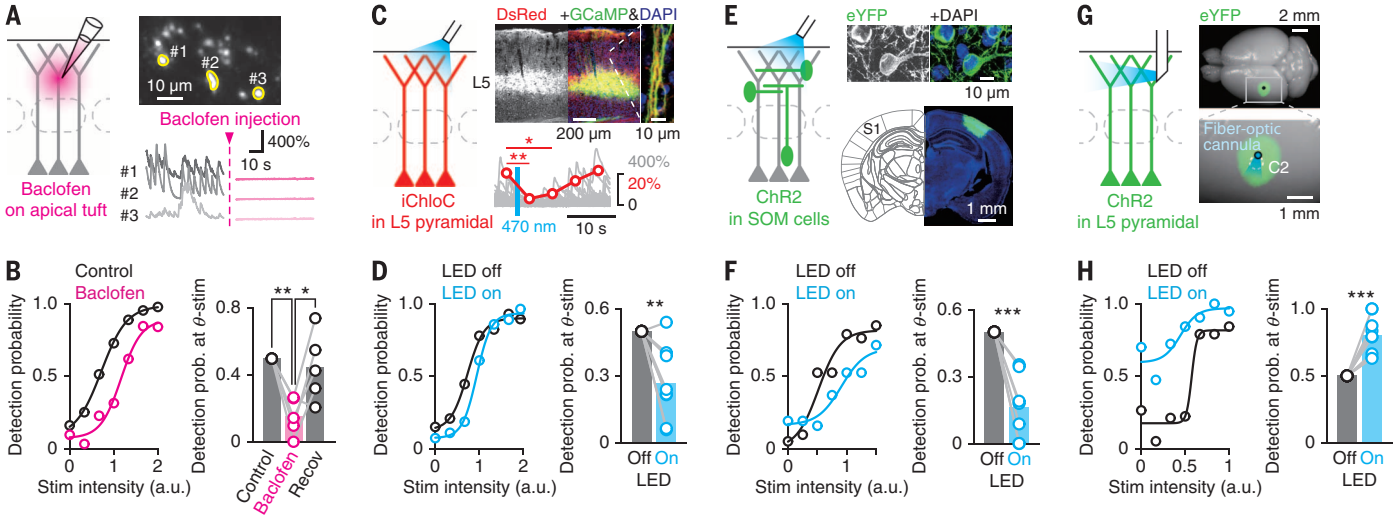

Fig. 4. Dendritic activity causally linked to perceptual detection threshold. (**A**) (Left) Schematic diagram of local application of $GABA_B$-receptor agonist, baclofen, to superficial layers of C2 barrel column. (Right) Ongoing Ca^{2+} activity in apical dendrites of GCaMP6s-expressing L5 neurons before and after the baclofen application. (**B**) (Left) Psychometric curves with and without local baclofen application. (Right) Effect of baclofen on the detection probability at the threshold stimulus intensity compared with control conditions [$n = 5$ mice, $^{**}P < 0.01$, $^{*}P < 0.05$, paired t test with Bonferroni's correction after one-way repeated-measures analysis of variance (ANOVA)]. (**C**) (Left) Optogenetic inactivation of apical dendrites of L5 neurons expressing iChloC. (Right) Brief illumination with blue light followed by a prolonged suppression of Ca^{2+} activity (bottom, $n = 120$ traces from 10 dendrites, $^{**}P < 0.01$, $^{*}P < 0.05$, Dunnett's test after ANOVA) in apical dendrites coexpressing iChloC and GCaMP6s (top). (**D**) (Left) Psychometric curves with [light-emitting diode (LED) on] and without (LED off) iChloC activation. (Right) Same as (B), with iChloC activation ($n = 8$ mice, $^{**}P = 5.8 \times 10^{-3}$, paired t test). (**E**) (Left) Controlling dendritic activity by activating dendrite-targeting SOM inhibitory cells. (Right) Specific expression of ChR2-eYFP in SOM cells in the C2 barrel column of S1. (**F**) Same as (B) and (D), with SOM-cell activation ($n = 7$ mice, $^{***}P = 9.2 \times 10^{-4}$, paired t test). (**G**) (Left) Optogenetic local activation of apical dendrites of L5 neurons expressing ChR2 using a fiberoptic cannula with a 45°-mirror tip. (Right) Expression of ChR2-eYFP in the C2 column and local photostimulation with the fiberoptic cannula. (**H**) Same as (B), (D), and (F), with ChR2 activation ($n = 9$ mice, $^{***}P = 2.1 \times 10^{-4}$, paired t test).

(both up and down) also significantly shifted the perceptual threshold in both directions (Fig. 4), suggesting a causal influence of apical calcium activity on perceptual detection.

The Ca^{2+} signals we recorded most likely represent the local activation of voltage-sensitive Ca^{2+} channels because single back-propagating action potentials (APs) and excitatory postsynaptic potentials (EPSPs) have little influence on apical dendritic Ca^{2+} signals (*26*, *27*). Although we cannot completely rule out the possibility that some of the dendritic Ca^{2+} signals were caused by bursts of back-propagating APs generated by proximal synaptic input (*28*), the fact that suppression or up-regulation of the dendrites specifically altered the animal's behavior argues against this interpretation and for the conclusion that they resulted from dendritic Ca^{2+} spikes (*2*), which is also consistent with elevated burst firing (*5*).

It has been suggested elsewhere that apical amplification via dendritic Ca^{2+} currents relates to conscious perception (*7*, *29*, *30*). The evidence presented in this study points in this direction because the task used, simple sensory detection, is often used to investigate conscious perception in humans (*13*, *31*, *32*). However, it is difficult to establish a relationship between apical amplification and perceptual experience in rodents. It has recently been shown that transcranial magnetic stimulation can noninvasively suppress Ca^{2+} activity in pyramidal dendrites (*33*), which may make it possible to test this mechanism in humans in the future.

REFERENCES AND NOTES

1. M. Murayama, M. E. Larkum, *Proc. Natl. Acad. Sci. U.S.A.* **106**, 20482–20486 (2009).
2. N. L. Xu *et al.*, *Nature* **492**, 247–251 (2012).
3. F. Gambino *et al.*, *Nature* **515**, 116–119 (2014).
4. J. Cichon, W. B. Gan, *Nature* **520**, 180–185 (2015).
5. M. E. Larkum, J. J. Zhu, B. Sakmann, *Nature* **398**, 338–341 (1999).
6. M. Larkum, *Trends Neurosci.* **36**, 141–151 (2013).
7. W. A. Phillips, A. Clark, S. M. Silverstein, *Neurosci. Biobehav. Rev.* **52**, 1–20 (2015).
8. D. J. Felleman, D. C. Van Essen, *Cereb. Cortex* **1**, 1–47 (1991).
9. K. S. Rockland, in *Extrastriate Cortex in Primates*, K. S. Rockland, J. H. Kaas, A. Peters, Eds. (Plenum Press, New York, 1997), pp. 243–293.
10. S. Sachidhanandam, V. Sreenivasan, A. Kyriakatos, Y. Kremer, C. C. Petersen, *Nat. Neurosci.* **16**, 1671–1677 (2013).
11. S. Manita *et al.*, *Neuron* **86**, 1304–1316 (2015).
12. S. E. Kwon, H. Yang, G. Minamisawa, D. H. O'Connor, *Nat. Neurosci.* **19**, 1243–1249 (2016).
13. B. Libet, W. W. Alberts, E. W. Wright Jr., B. Feinstein, *Science* **158**, 1597–1600 (1967).
14. J. F. Corso, *Psychol. Bull.* **60**, 356–370 (1963).
15. R. P. Rao, D. H. Ballard, *Nat. Neurosci.* **2**, 79–87 (1999).
16. M. C. Stüttgen, C. Schwarz, *Nat. Neurosci.* **11**, 1091–1099 (2008).
17. D. H. O'Connor, S. P. Peron, D. Huber, K. Svoboda, *Neuron* **67**, 1048–1061 (2010).
18. L. M. Palmer *et al.*, *Science* **335**, 989–993 (2012).
19. G. Doron, M. von Heimendahl, P. Schlattmann, A. R. Houweling, M. Brecht, *Neuron* **81**, 653–663 (2014).
20. E. Pérez-Garci, M. E. Larkum, T. Nevian, *J. Physiol.* **591**, 1599–1612 (2013).
21. J. Wietek *et al.*, *Sci. Rep.* **5**, 14807 (2015).
22. G. Silberberg, H. Markram, *Neuron* **53**, 735–746 (2007).
23. M. Murayama *et al.*, *Nature* **457**, 1137–1141 (2009).
24. L. J. Gentet *et al.*, *Nat. Neurosci.* **15**, 607–612 (2012).
25. M. Carandini, A. K. Churchland, *Nat. Neurosci.* **16**, 824–831 (2013).
26. F. Helmchen, K. Svoboda, W. Denk, D. W. Tank, *Nat. Neurosci.* **2**, 989–996 (1999).
27. M. Murayama, E. Pérez-Garci, H. R. Lüscher, M. E. Larkum, *J. Neurophysiol.* **98**, 1791–1805 (2007).
28. M. E. Larkum, K. M. Kaiser, B. Sakmann, *Proc. Natl. Acad. Sci. U.S.A.* **96**, 14600–14604 (1999).
29. T. Bachmann, *Front. Psychol.* **6**, 1947 (2015).
30. K. Meyer, *Anesthesiology* **122**, 1415–1431 (2015).
31. S. Palva, K. Linkenkaer-Hansen, R. Näätänen, J. M. Palva, *J. Neurosci.* **25**, 5248–5258 (2005).
32. B. Pleger, A. Villringer, *Prog. Neurobiol.* **103**, 76–97 (2013).
33. S. C. Murphy, L. M. Palmer, T. Nyffeler, R. M. Müri, M. E. Larkum, *eLife* **5**, e13598 (2016).

ACKNOWLEDGMENTS

We thank J. Sigl-Glöckner for assistance with histology; M. Suzuki for assistance with transgenic animals; J. S. Wiegert for viral constructs; and W. A. Phillips for comments and discussions on the manuscript. This study was supported by the Deutsche Forschungsgemeinschaft (EXC NeuroCure, LA 3442/3-1, SPP1665, SFB1078 B2), European Union Horizon 2020 Research and Innovation Programme (under grant agreement numbers 72070/HBP SGA1 and 670118/ERC ActiveCortex), the Japan Society for the Promotion of Science, the Uehara Memorial Foundation, and the Kanae Foundation for the Promotion of Medical Science. N.T. and M.E.L. conceived the project and designed the experiments. N.T. performed all the experiments and data analysis. N.T. and M.E.L. wrote the paper. T.G.O. and P.H. provided the viral construct iChloC. Original data are kept on local hard drives (with backups). P.H. is Hertie Senior Professor for Neuroscience. Processed data for this study (including extracted calcium traces) are additionally kept and curated on servers of the Charité Universitätsmedizin–Berlin. The authors declare that they have no competing financial interests.

SUPPLEMENTARY MATERIALS

www.sciencemag.org/content/354/6319/1587/suppl/DC1
Materials and Methods
Figs. S1 to S6
References (*34*–*36*)

20 July 2016; accepted 23 November 2016
10.1126/science.aah6066

Active cortical dendrites modulate perception
Naoya Takahashi, Thomas G. Oertner, Peter Hegemann and Matthew E. Larkum (December 22, 2016)
Science **354** (6319), 1587-1590. [doi: 10.1126/science.aah6066]

Editor's Summary

Now you feel it, now you don't

What determines the detection of a sensory stimulus? To address this question, Takahashi *et al.* combined in vivo two-photon imaging, electrophysiology, optogenetics, and behavioral analysis in a study of mice. Calcium signals in apical dendrites of pyramidal neurons in the somatosensory cortex controlled the perceptual threshold of the mice's whiskers. Strong reduction of dendritic calcium signaling impaired the perceptual detection threshold so that an identical stimulus could no longer be noticed.

Science, this issue p. 1587

Science (print ISSN 0036-8075; online ISSN 1095-9203) is published weekly, except the last week in December, by the American Association for the Advancement of Science, 1200 New York Avenue NW, Washington, DC 20005.